

Modelling and Removing the Gradient Artefact using a Gradient Model Fit (GMF)

Glyn S Spencer¹, Karen J Mullinger¹, Andrew Peters¹, and Richard Bowtell¹
¹SPMMRC, School of Physics and Astronomy, University of Nottingham, Nottingham, Nottinghamshire, United Kingdom

Introduction: EEG data recorded in the MR scanner is affected by a number of artefacts. The largest of these is the gradient artefact (GA) caused by temporally-varying magnetic field gradients. Average Artefact Subtraction (AAS), which is the most widely used method for GA correction [1], requires the GA to be highly stable across repeated slice acquisitions in multi-slice EPI. This assumption is violated when small changes in subject position occur during a study [2], leaving residual artefacts that can be much larger than neuronal signals. Head movements often occur during EEG/fMRI experiments; therefore a method of GA correction whose performance is unaffected by such movements is desirable. Modelling work has shown that the GA is formed from a linear superposition of the individual artefacts generated by the waveforms applied on the orthogonal read, phase and slice gradient axes [3]. Changes in the GA resulting from variations in the position of the head and/or EEG leads can thus be viewed as resulting from changes in the relative weighting of the superposed artefact waveforms from the different gradient channels. Here we verify this concept and use it to introduce a novel GA correction method, which is based on a gradient model fit (GMF) aimed at improving GA correction in data affected by head movement.

Methods: Models of the GA for the individual gradient axes can be generated by recording the GA waveforms produced during an EPI sequence in which two of the three gradient waveforms (read, phase or slice) in turn are nulled. This leads to the production of three models per lead which can be linearly superposed to form the full GA. These models can be adaptively-fitted to the GAs produced during each slice acquisition of a normal EEG/fMRI experiment and the fitted model then subtracted from the data. Changes in the GA after movement are reflected in changes in the weightings of the different models' contributions to the fitted GA, yielding a continuously good fit without requiring any additional information about the timing of subject movements. The very different temporal characteristics of the GA models and signals resulting from neuronal activity mean that subtraction of the GMF should leave the latter unattenuated. During our experiments we identified an unexpected additional artefact component which was generated by the RF. This was isolated by recording during an EPI sequence in which all gradient waveforms were nulled and found to be associated with application of the RF pulse and the RF coil gating between slice selection and signal acquisition (see Fig. 1). This RF artefact component was also therefore included in the modelling.

EEG recordings were made in a Philips Achieva 3T MR scanner using a Brain Products EEG system (32 channel cap, Brain Amp MRplus, 5 kHz sampling rate). Low-pass filtering was applied with a cut-off frequency of 1 kHz to ensure accurate characterisation of the high frequency components of the GA. Amplifier saturation was avoided by careful positioning of the phantom/subject [4]. Synchronisation of the scanner clocks [5] was imperative for accurate sampling of the artefact waveforms to ensure that the model waveforms matched the GA from the full EPI sequence. An EPI pulse sequence was customized so that the four artefact waveforms could be individually recorded in the initial repeats of the multi-slice EPI acquisition. In this way, 20 repeats of each of these waveforms (spanning one slice acquisition) were acquired prior to acquisition of 50 volumes of standard EPI data. Recordings were acquired from a conducting, head-sized spherical agar phantom and from a healthy human subject. During the standard EPI acquisition (5 slices, 36×36 matrix, 7 mm isotropic resolution, TR/TE = 2000/35ms) the phantom was moved by <1.6mm and held in the new position. Similarly, the subject was asked to adjust their position during acquisition. These movements were <1.5 mm thus simulating the GA changes that are likely to occur in fMRI experiments.

Analysis: Models of the three GA components and the RF artefact on each channel were formed in Matlab by averaging the 20 repeats acquired at the beginning of the sequence (Fig. 1). The models were then adaptively fitted to each full EPI slice artefact in the EEG data using GLMs which were focused on regions where specific artefact components were maximal. To fit the Slice gradient and RF models the period of slice selection was used and a GLM comprising the models, a DC offset, linear, centred quadratic and cubic functions (which modelled the changes in baseline due to other signals such as the pulse artefact, movement artefact or neuronal activity) was employed. A pseudo-inverse matrix was calculated and used to estimate the scaling parameters for these components. The model waveforms spanning the entire GA period were then scaled and subtracted from the EEG data for the corresponding slice. This process was then repeated for the Read and Phase gradient models focusing on the read-out portion of the GA. AAS was also applied to the raw EEG data using Analyzer2 (Brain Products) and a template formed by averaging over all slice artefacts, so as to provide a standard for evaluating the performance of the GMF method. Additionally AAS was applied to the data after GMF to determine if any residual GA could be further attenuated. To provide a measure of performance of each correction method the root mean square (RMS) amplitude of the residual artefacts was averaged over channels for all frequency bands and also after filtering to focus upon GA at frequencies greater than 80 Hz, whose correction can be problematic using AAS.

Results and Discussion: Figure 2A&B show the GA produced on a single channel by slice acquisitions before and after movement of the phantom. The GA shows significant changes in form after the movement, but is well characterised by the GMF in both plots. The changes in the GA after movement are mainly reflected in the Read/Slice model weightings changing by $\times 1.21/0.86$. This demonstrates that even when movements occur the GA can still be represented as a linear superposition of the gradient and RF artefact components [3]. Figure 2C&D show that GMF performs similarly well before and after movement in eliminating the GA, but that the performance of AAS is compromised by the presence of the movement. The improvement in artefact correction when using GMF compared with AAS on the phantom is also reflected in the entire data set (Table 1) with a greater improvement occurring in the higher frequency range (>80 Hz) which can currently be difficult to study using AAS. A further improvement in the correction is seen if AAS is employed after GMF suggesting that the fitting has taken out the variability across slices and other residuals can then be removed with AAS. The results from data acquired on a subject show no significant improvement from using GMF or GMF+AAS versus AAS on the unfiltered data however an improvement is seen in the higher frequency bands. This difference in performance may be due to the dominance of the pulse artefact and neuronal signals in the GA-corrected data. Our results show that GMF potentially offers better performance than conventional GA correction methods particularly in high frequency bands. This could be highly beneficial for investigation of gamma frequency (30-150 Hz) neuronal activity.

References: [1] Allen *et al.* Neuroimage 12:230, 2000, [2] Moosmann *et al.* Neuroimage 45:1144, 2009, [3] Yan *et al.* Neuroimage 46:459, 2009, [4] Mullinger *et al.* Neuroimage 54:1942, 2011, [5] Mandelkow *et al.* Neuroimage 32:1120, 2006

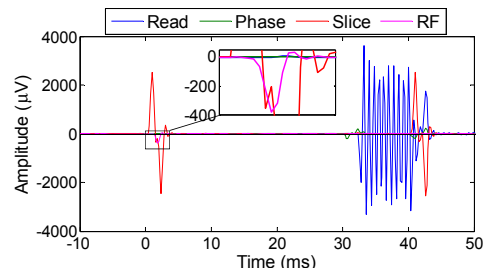


Figure 1: Model formed by the superposition of artefacts from the orthogonal gradients from data recorded on a phantom. Inset clearly shows the presence of RF artefact.

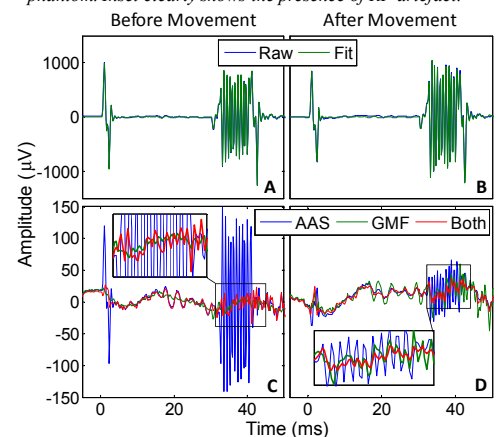


Figure 2: Slice GA from channel Fp2 before (A) and after (B) phantom movement (blue) with model fitted to each slice (green). C and D show the residual GA for these slices after artefact correction using the three methods described.

	Raw (μV)	AAS (μV)	GMF (μV)	GMF and AAS (μV)
Unfiltered	470 ± 40	50 ± 3	47 ± 4	46 ± 4
	330 ± 30	62 ± 4	62 ± 4	62 ± 4
>80 Hz	460 ± 40	21 ± 1	11.0 ± 0.8	9.2 ± 0.6
	320 ± 30	10.3 ± 0.6	10.0 ± 0.6	9.4 ± 0.5

Table 1: The mean RMS of the EEG data over all channels before (raw) and after GA correction using each algorithm.